III International Conference on Particle-based Methods – Fundamentals and Applications
PARTICLES 2013
M. Bischoff, E. Oñate, D.R.J. Owen, E. Ramm & P. Wriggers (Eds)

PARTICLE-BASED MODEL OF CELLULAR MORPHOGENESIS IN BUDDING YEAST

MARCIN LEDA[1], SATOSHI OKADA[2], ERFEI BI[2], YVES BARRAL[3] AND ANDREW B. GORYACHEV[1]

[1]Centre for System and Synthetic Biology, University of Edinburgh, Edinburgh EH9 3JD, UK
[2]Department of Cell and Developmental Biology, Perelman School of Medicine, University of Pennsylvania, Philadelphia, PA 19104, USA
[3]Instiute of Biochemistry, ETH Zurich, Zurich, Switzerland

mleda@staffmail.ed.ac.uk, Andrew.Goryachev@ed.ac.uk

Key words: Cellular morphogenesis, Lagrangian particle method, Level Set method, Reaction-Diffusion on Surfaces.

Abstract
We apply Lagrangian particle method combined with the level-set method to model morphogenesis of budding yeast on the subcellular level. We model the biochemical reactions, anisotropic diffusion, membrane-cytoplasmic transport of proteins and introduction of new membrane material (exocytosis) that occur on the plasma membrane. Exocytosis results in protrusion of the membrane surface. Hence, to model these phenomena we need to solve a system of reaction-diffusion-advection equations on the evolving surface.

MODEL

Our biological system is composed of the plasma membrane enclosing a homogeneous cytoplasmic compartment. Chemical reactions, diffusion and transport from the cytoplasm may occur on the membrane. The surface of the membrane may move due to insertion of new membrane material by exocytosis process. The spatio-temporal rate of exocytosis is believed to be defined by the concentrations of proteins on the membrane.

From the biochemical point of view, the main molecules are signaling GTP-binding protein Cdc42 (a small Rho GTPase), its regulators (activating GEF and inactivating GAP) and septin polymer (P) formed from the monomers recruited to the membrane by the active form of $Cdc42^{GTP}$ (Fig. 1) [1].

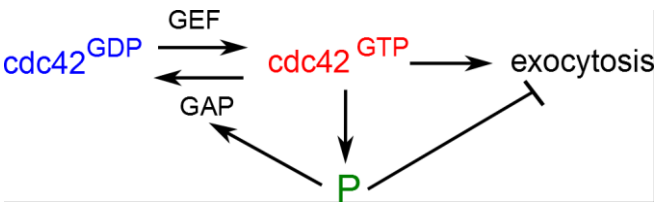

Figure 1. Reaction network scheme.

We solve reaction-diffusion-advection system on the evolving surface *S*.

$$\frac{\partial c_i}{\partial t} + \nabla_S(\mathbf{u}c_i) = R_i(\mathbf{c},\mathbf{b}) + \nabla_S(D_i(\mathbf{c})\nabla_S c_i) \quad \text{i=1, ... , } n \quad (1)$$

Diffusion tensors may be concentration dependent. We assume the simplest exponential dependence for the diffusion coefficients of species on the concentration of septin polymer P

$$D_i = \left(D_{i,0} - D_{i,1}\right)e^{-P/K_d} + D_{i,1} \quad (2)$$

where K_d, $D_{i,1}=D_{i,0}/d_f$ and $d_f>0$ are the measures of the strength of diffusion barrier imposed by septin. $D_{i,0}$=0.01 μm^2/s corresponds to diffusion coefficient in the absence of diffusion barrier.

Concentrations in the homogeneous cytosol enclosed by surface *S* are described by the following ordinary differential equations

$$\frac{db_i}{dt} = R_i(\mathbf{c},\mathbf{b}) \qquad \text{i=1, ... , } n_c. \quad (3)$$

Our system possess also constant integrals resulting from mass conservation of proteins

$$F_i(\int \mathbf{c}dS\,, \mathbf{b}) = I_{i,tot} \quad \text{i=1, ... , } m$$

For example, for GEF protein we have

$$\int_S ([GEF] + [GEF{:}\,cdc42^{GTP}])dA + V_{cytosol}[GEF]_{cytosol} = V_{cytosol}[GEF]_{total}$$

Membrane surface is represented by the level-set function φ. Exocytosis is modelled as movement of this function with a normal velocity $\boldsymbol{u}$ dependent on the species concentrations on the membrane (Cdc42^{GTP} and P, in particular).

$$\frac{\partial \varphi}{\partial t} + \mathbf{u}(\boldsymbol{c})\nabla\varphi = 0 \quad (4)$$

Based on known biological facts we use the following formula for exocytosis rate

$$r = r_{exo}\frac{f}{A^{-1}\int_S f dA}$$

$$f = \frac{c^2_{\mathrm{cdc42^{GTP}}}}{1 + c_{\mathrm{P}}/K_P}$$

where f is a function of local concentration of species, A is the membrane surface and r_{exo} is the total rate of exocytosis (number of exocytic vesicles introduced in 1 sec) in the case of a uniform cell growth. If exocytosis is not polarized (uniform), the surface of a spherical cell grows as $\dot{A} = 8\pi r|\mathbf{u}|$ and $\dot{A}$ is equal to $r_{exo}A_v$ where A_v is the area of an exocytic vesicle. In this way we may translate the rate of exocytosis into the surface velocity $\boldsymbol{u}$.

METHODS

Equations (1) and (4) are discretized on the particles localized at the nodes of a uniform rectangular mesh.

$$\frac{d\boldsymbol{x}_p}{dt} = \boldsymbol{u}(\boldsymbol{x}_p, t) \quad (5a)$$

$$\frac{d\boldsymbol{n}_p}{dt} = V_p R(\boldsymbol{c}) + V_p \nabla_S^h \left(\boldsymbol{D} \nabla_S^h \boldsymbol{c}_p\right) \quad (5b)$$

$$\frac{d\varphi_p}{dt} = 0 \quad (5c)$$

$$\frac{dV_p}{dt} = V_p \nabla_S^h \boldsymbol{u}(\boldsymbol{x}_p, t) \quad (5d)$$

where $\boldsymbol{n}_p$ is the mass of species in particle p, ∇_S^h is the discretized version of the gradient operator and $\boldsymbol{x}_p$ and V_p are the position and volume of particle p, respectively.
We apply the particle strength exchange (PSE) method [2] combined with the level set method to simulate anisotropic diffusion on an evolving surface. The level set function is computed in a narrow band of radius k. The surface diffusion operator is obtained by projecting the true surface operator to the 3D narrow band of radius k_d. The method is shortly described in the flow chart in Fig. 2. In mathematical terms it may be presented as follows:

1) Re-initialization of the level-set function by solving equation

$$\|\nabla\varphi\|_2 = 1 \quad (6a)$$

using group marching method (GMM) of order 2 or by solving an equivalent equation

$$\frac{\partial\varphi}{\partial\tau} + sgn(\varphi)(\nabla\varphi\nabla\varphi) = 0 \quad (6b)$$

using WENO Hamiltonian Jacobi solver in 3D tube of radius k.

2) Extension of concentration from the narrow tube of radius k_d to narrow tube of radius k by solving equation

$$\nabla c \nabla\varphi = 0 \quad (4a)$$

using GMM of order 2 or by solving equivalent equation

$$\frac{\partial\varphi}{\partial\tau} + sgn(\varphi)(\nabla\varphi\nabla u) = 0 \quad (4b)$$

using WENO Hamiltonian Jacobi solver.

3) Computation of Laplacian on the surface

$$\frac{1}{\|\nabla\varphi\|_2} \nabla(\boldsymbol{T}\boldsymbol{D}\nabla c) \quad (6a)$$

using projection tensor

$$\boldsymbol{T} = \left(1 - \frac{\nabla\varphi \otimes \nabla\varphi}{\|\nabla\varphi\|_2^2}\right) \|\nabla\varphi\|_2 \quad (6b)$$

where all differential operators are now computed in a 3D narrow band of radius k_d.

4) Computation of the 3D diffusional tensor using PSE method with 2nd order B-spline-4 kernel [3].

$$\eta(s)=\begin{cases}\frac{3}{2}s^3-\frac{5}{2}s^2+1 & 0\le s\le 1\\ -\frac{1}{2}s^3+\frac{5}{2}s^2-4s+2 & 0\le s\le 2\\ 0 & s>2\end{cases} \quad (7)$$

where $s=x/h$. Anisotropic Laplacian in Eq. (6a) is discretized as follows

$$\nabla(\widetilde{\boldsymbol{D}}\nabla\boldsymbol{c})\approx\epsilon^{-4}\left[\sum_{q=1}^{N}V_q\left(c_q-c_p\right)\eta(\boldsymbol{x}_p-\boldsymbol{x}_q)\sum_{i,j}^{3}M_{i,j}\left(\boldsymbol{x}_p,\boldsymbol{x}_q\right)(\boldsymbol{x}_p-\boldsymbol{x}_q)_i(\boldsymbol{x}_p-\boldsymbol{x}_q)_j\right] \quad (8)$$

where $\widetilde{\boldsymbol{D}}=\boldsymbol{TD}$ and **M** is as proposed by Degond and Mas-Gallic [4]

$$\boldsymbol{M}\left(\boldsymbol{x}_p,\boldsymbol{x}_q\right)=\frac{1}{2}\left(\boldsymbol{m}\left(\boldsymbol{x}_p\right)+\boldsymbol{m}\left(\boldsymbol{x}_q\right)\right) \quad (9a)$$

$$\boldsymbol{m}(x)=\widetilde{\boldsymbol{D}}(x)-\frac{1}{5}Tr\left(\widetilde{\boldsymbol{D}}(x)\right)\mathbf{1} \quad (9b)$$

Spatial dependence of the diffusion tensor in Eq. (9b) allows us to introduce here concentration dependence of the diffusional tensor.

5) Map particle mass and level-set function to rectangular mesh using partition of the unity kernel (7)

$$n_p^{new}=V_p^{new}\sum_{q=1}^{N}n_p^{old}\,\eta\left(\boldsymbol{x}_q^{new}-\boldsymbol{x}_q^{old}\right)$$

$$\varphi_p^{new}=\frac{\sum_{q=1}^{N}V_p^{old}\varphi_p^{old}\,\eta\left(\boldsymbol{x}_q^{new}-\boldsymbol{x}_q^{old}\right)}{\sum_{q=1}^{N}V_p^{new}\,\eta\left(\boldsymbol{x}_q^{new}-\boldsymbol{x}_q^{old}\right)}$$

where $V_p^{new}=h^3$ and h is the rectangular mesh size. System (5) is solved by explicit time-stepping method (STS) with nine steps [5]. Whole algorithm is coded using PPM parallel particle mesh library [6] procedures.

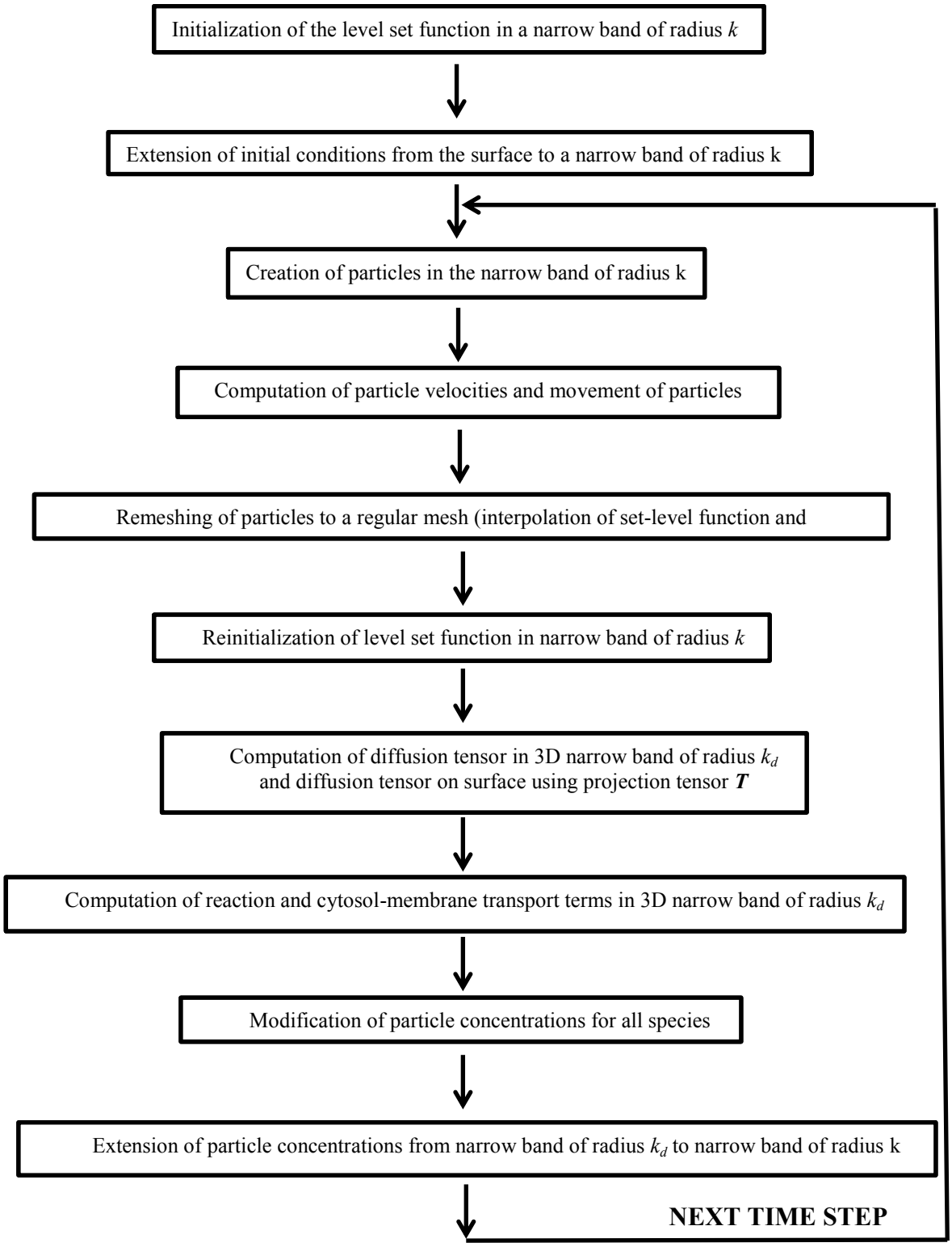

Figure 2. Flow chart of the method.

RESULTS

Initial conditions are zero concentrations for all species on the spherical membrane of radius 2μm which correspond to an average size of an unbudded yeast cell. Table 1 presents typical numerical parameters used in our simulations. Because due to transport from the cytosol the total mass on the membrane increases, we found GMM method as better extension method for our system.

Parameter	Value
spatial step ($\Delta x=\Delta y=\Delta z=h$)	0.04 μm
ε (kernel radius)	$2h$
c_f (cut-off for particle strength exchange)	$4h$
k (level set tube radius)	$3.5c_f$
k_d (PSE tube radius)	$2.5c_f$
N_p (number of particles)	200000
NI (number of iteration in H-J solver)	100
tol (solution change in subsequent iterations)	10^{-3}

Table 1. Parameters of the computational method.

Cytosol-membrane transport terms are computed for particles which are inside tube of radius k_d where diffusional operator is computed. This guarantees conservation of the protein amount because PSE algorithm conserves mass. However, this causes dependence of simulation results on the numerical parameters. It may be avoided by the proper choice of volume ratio between the cytosolic and membrane compartments $v=V_c/V_m$. For example, the number of GEF proteins is conserved according to the following equation

$$\sum_{i=1}^{N_p} V_i([GEF]_i + [GEF{:}\,cdc42^{GTP}]_i) + V_{cytosol}[GEF]_{cytosol} = V_{cytosol}[GEF]_{total}$$

where N_p and V_i are the number and volumes of particles, respectively. Because we used particles localized at the nodes of rectangular mesh, all V_i are equal to V_p and the mass conservation equation reads

$$\frac{1}{N_p v}\sum_{i=1}^{N_p} ([GEF]_i + [GEF{:}\,cdc42^{GTP}]_i) + [GEF]_{cytosol} = [GEF]_{total}$$

v in typical yeast cell is approximately equal to 100 because not entire volume enclosed by the membrane is available for cytosol.

Formation of the septin ring plays crucial role in the asymmetric cell division of budding yeast. It determines the identity of budding new cell and separates plasma membranes of mother and daughter cells [7]. Using genetic manipulation and live cell imaging, we demonstrated that impaired exocytosis results in the defective formation of the septin ring [8]. In the absence of exocytosis, septins form a solid cap (or a cloud) and the transition from cap to ring (ring opening) may not take place at all. With weak exocytosis, opening of the ring is delayed or transient.

In complete agreement with experimental data, our simulations show that the first stage of ring formation is a septin cloud (green colour in Fig. 3a) which co-localizes with the $cdc42^{GTP}$ cluster (red colour). Then, if intensity of exocytosis is high enough, the ring opens as a result of new material introduction (Fig. 3b). Moreover, if the spatial profile of exocytosis is not sufficiently focused, a broad protrusion is formed instead of the ring (Fig. 4a). Figures 4a and 4b show how different spatial profiles of surface expansion velocity may create different yeast cell morphologies: broad protrusion or bud neck, respectively.

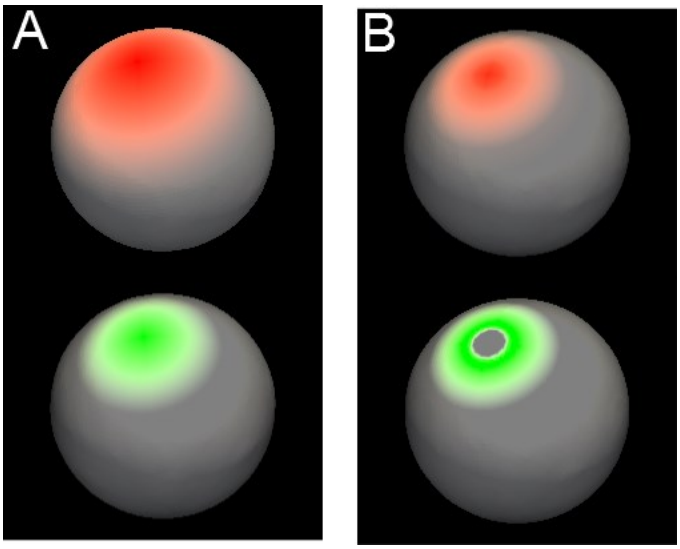

Figure 3. Septin polymer P (green) is initially recruited as cloud by $cdc42^{GTP}$ cluster (red) (A). Then exocytosis opens the septin ring (B).

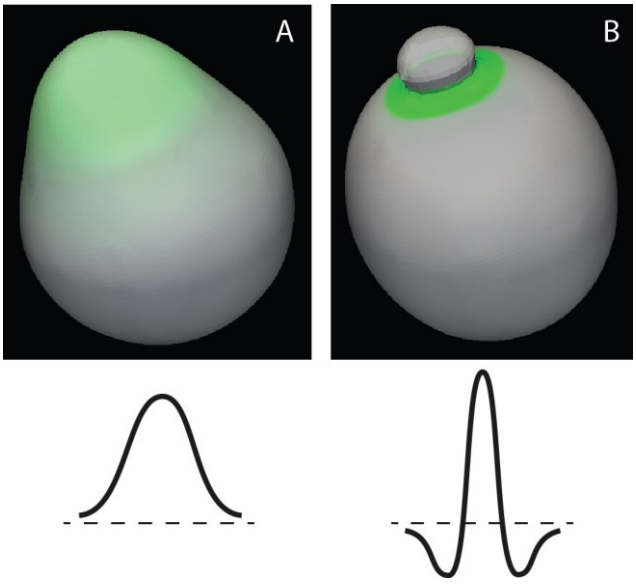

Figure 4. Different profiles of expansion velocity (bottom) create different cell morphologies: broad protrusion (A) or bud neck (B). Only concentration of septin polymer (green) is shown.

CONCLUSIONS

The most striking difference between non-biological and biological reaction-diffusion systems is the growth of the latter. We use deterministic Lagrangian particle method to study the influence of growth on the formation of polarity patterns in a budding yeast cell. We model early stages of morphogenesis (polarization and septin ring formation). In the future work we are going to introduce a biomechanical description of the membrane which may allow us to study later stages of cell division including cytokinesis. Another straightforward modification of the method is to use stochastic description for the chemical reactions and the cytosol-membrane transport processes.

REFERENCES

[1] Goryachev, A. B., and Pokhilko, A. V. Dynamics of Cdc42 network embodies a Turing-type mechanism of yeast cell polarity. *FEBS Lett* (2008) **582**: 1437-1443.

[2] Bergdorf, M., Sbalzarini, I. F., and Koumoutsakos, P. A Lagrangian particle method for reaction-diffusion systems on deforming surfaces. *J. Math. Biol.* (2010) **61**: 649-663.

[3] Monaghan, J. J., Extrapolating B splines for interpolation. *J. Comp. Physics* (1985) **6**: 253–262.

[4] Degond, P. and Mas-Gallic S., The weighted particle method for convection-diffusion equations. Part 2: The Anisotropic Case. *Mathematics of Computation*. (1989) **53**: 509-525.

[5] Alexiades, V., Amiez, G., and Gremaud, P.A Super-time-stepping acceleration of explicit schemes for parabolic problems. *Communications in Numerical Methods in Engineering*. (1996) **12**: 31-42.

[6] Sbalzarini, I. F., Walther, J. H., Bergdorf M., Hieber S. E., Kotsalis, E. M., Koumoutsakos, P. E., PPM A highly efficient parallel particle mesh library for the simulation of continuum systems. *J. Comp. Physics* (2006) **215**: 566-588.

[7] Caudron, F., and Barral, Y. Septins and the lateral compartmentalization of eukaryotic membranes. *Dev. Cell* (2009) **16:** 493-506.

[8] Okada S., Leda, M., Hanna, J., Savage, N. S., Bi, E., and Goryachev, A. B., Daughter cell identity emerges from the interplay of Cdc42, septins and exocytosis. *Dev. Cell* (2013) *in press*